

ORIGINAL ARTICLE

Dystroglycan on Radial Glia End Feet Is Required for Pial Basement Membrane Integrity and Columnar Organization of the Developing Cerebral Cortex

Timothy D. Myshrell, DVM, Steven A. Moore, MD, PhD, Adam P. Ostendorf, MD, Jakob S. Satz, PhD, Tom Kowalczyk, BS, Huy Nguyen, MS, Ray A.M. Daza, BS, Charmaine Lau, BS, Kevin P. Campbell, PhD, and Robert F. Hevner, MD, PhD

Abstract

Interactions between the embryonic pial basement membrane (PBM) and radial glia (RG) are essential for morphogenesis of the cerebral cortex because disrupted interactions cause cobblestone malformations. To elucidate the role of dystroglycan (DG) in PBM-RG interactions, we studied the expression of DG protein and *Dag1* mRNA (which encodes DG protein) in developing cerebral cortex and analyzed cortical phenotypes in *Dag1* CNS conditional mutant mice. In normal embryonic cortex, *Dag1* mRNA was expressed in the ventricular zone, which contains RG nuclei, whereas DG protein was expressed at the cortical surface on RG end feet. Breaches of PBM continuity appeared during early neurogenesis in *Dag1* mutants. Diverse cellular elements streamed through the breaches to form leptomeningeal heterotopia that were confluent with the underlying residual cortical plate and contained variably truncated RG fibers, many types of cortical neurons, and radial and intermediate progenitor cells. Nevertheless, layer-specific molecular expression seemed normal in heterotopic neurons, and axons projected to appropriate targets. Dendrites, however, were excessively tortuous and lacked radial orientation. These findings indicate that DG is required on RG end feet to maintain PBM integrity and suggest that cobblestone malformations involve disturbances of RG structure, progenitor distribution, and dendrite orientation, in addition to neuronal “overmigration.”

Key Words: Cerebral cortex, cobblestone malformation, dystroglycan, leptomeningeal heterotopia, lissencephaly.

From the Departments of Comparative Medicine (TDM) and Neurological Surgery (TK, CL, RFH), University of Washington; Seattle Children's Research Institute (RAMD, RFH), Seattle, Washington; and Departments of Pathology (SAM, APO, JSS, HN), Molecular Physiology and Biophysics (JSS, KPC), Internal Medicine (KPC), and Neurology (KPC), University of Iowa, Iowa City, Iowa.

Send correspondence and reprint requests to: Robert F. Hevner, MD, PhD, Seattle Children's Research Institute, 1900 Ninth Ave, Seattle, WA 98101; E-mail: rhevner@uw.edu

Timothy D. Myshrell is now with the Lerner Research Institute, Cleveland, Ohio. Kevin P. Campbell is an investigator of the Howard Hughes Medical Institute.

This work was supported by Grant 5 T32 RR07019 (to Timothy D. Myshrell), Grant R01 NS050248-04 (to Robert F. Hevner), Grant R21 NS041407 (to Steven A. Moore), and Grant U54 NS053672 (to Steven A. Moore and Kevin P. Campbell) from the National Institutes of Health.

INTRODUCTION

Neuronal overmigration defects are a group of malformations characterized by ectopic migration of neurons beyond the glia limitans into the meningeal spaces and cobblestone lissencephaly (1–5). Depending on the extent and severity of the defects, neuronal overmigration can manifest pathologically as a nodular, polymicrogyric, or narrow residual cortex (6). In syndromes of cobblestone malformations with congenital muscular dystrophy (CMD), such as muscle-eye-brain disease, Walker-Warburg syndrome, and Fukuyama congenital muscular dystrophy, the defect is not with neurons but with signaling interactions between the pial basement membrane (PBM) and radial glia (RG) processes (7–12). Direct PBM-RG interactions are necessary to maintain PBM integrity, which is in turn essential to smoothly delimit the brain surface and maintain the glia limitans (13). Deficient PBM-RG signaling leads to ruptures in the PBM, thus opening a permissive environment for neuronal overmigration (13).

The PBM-RG signaling is mediated by extracellular matrix (ECM) glycoproteins, particularly laminin, binding to transmembrane receptors expressed on RG end feet (14). The key laminin receptors transducing this interaction include integrins and a brain form of the dystrophin glycoprotein complex. Generally, in the human cobblestone malformations associated with CMDs, ECM receptor signaling is attenuated as a result of deficient glycosylation of α -dystroglycan (α -DG), the laminin-binding subunit of DG, a key glycoprotein component of the dystrophin glycoprotein complex (15–21). Extensive glycosylation is essential for α -DG activities, including laminin binding (14, 18, 22). Thus, whereas most cobblestone malformations in humans are linked to mutations in protein glycosylation genes, the key effect is to perturb functions of α -DG related to PBM-RG signaling. Accordingly, syndromes of cobblestone malformations with CMD are considered subtypes of dystroglycanopathy, a broad group of CMDs and limb-girdle muscular dystrophies, which may or may not be associated with brain and ocular malformations (OMIM No. 253800). The pathogenesis of cobblestone malformations has been studied in several mouse models produced by targeted mutations of genes involved in PBM-RG signaling mediated by integrins and DG. Some of these models have revealed surprisingly complex effects, involving multiple neurodevelopmental

abnormalities, in addition to neuronal overmigration and laminar disorganization. For example, in mice with a laminin mutation that interfered with binding to nidogen (an ECM-organizing molecule), the developing cerebral cortex showed ectopic RG progenitor proliferation, widespread retraction of RG end feet, focal RG fiber extension into heterotopia, gaps in the distribution of Cajal-Retzius (CR) cells, and spontaneous hemorrhages (23). Some of the same defects were also reported in mutants lacking β 1-integrin, α 6-integrin, glycosyltransferases that posttranslationally modify DG, or signaling molecules such as FAK, a nonreceptor tyrosine kinase, and ILK, a nonreceptor serine/threonine kinase, both of which are activated by integrin signaling (7–9, 22, 24–28).

In the present study, our goal was to investigate the pathogenesis of cobblestone malformations in dystroglycanopathy. Toward this goal, we studied mice with conditional inactivation of the DG gene, *Dag1*, in the embryonic CNS. This was accomplished by Cre-mediated recombination using *Nestin-Cre* expressed in central neural stem cells to inactivate a floxed *Dag1* allele in the embryonic brain and spinal cord (29). Conditional inactivation was necessary because complete *Dag1* null mutants die during early gastrulation stages (30). Previous studies using *Gfap-Cre* or *Mox2-Cre* to inactivate floxed *Dag1* in RG progenitors or epiblast derivatives, respectively, have shown that adult mice lacking central DG indeed develop a severe cobblestone malformation characterized by abnormal cortical layering, meningeal heterotopia, and fusion of the interhemispheric fissure (14, 31). These previous studies confirmed the importance of DG in brain development, but many questions have remained. The most fundamental of these is which cell types in the embryonic cortex express DG? Given the presumed role of DG in PBM-RG signaling, it has been assumed that DG is expressed by RG cells, but this has never been conclusively demonstrated. Other questions include what are the effects of central DG deficiency on progenitor cells and RG fibers in the embryonic cortex? And how are the distribution and connections of cortical pyramidal neurons and interneurons affected?

In the present study, we verified that *Dag1* mRNA is indeed expressed by RG cells in the embryonic ventricular zone (VZ), whereas DG protein is localized to RG end feet in contact with the PBM. We also found that *Dag1* inactivation led to ectopic proliferation of RG progenitors and intermediate progenitor cells (IPCs), proliferation of progenitors within the VZ and subventricular zone (SVZ), despite RG fiber anomalies, and overmigration of all cortical neuron types into the leptomeninges. Despite severe dyslamination and abnormal dendrite orientation, ectopic pyramidal neurons established axonal connections with distant cortical and subcortical targets, consistent with the view that axon pathfinding does not require laminar organization or DG signaling. Our findings reveal that the pathogenesis of cobblestone malformation in dystroglycanopathy is more complex than previously understood.

MATERIALS AND METHODS

Mice

Nestin-Cre/DG-null mice were generated, as previously described (29), by breeding nestin-Cre mice (Jackson Labo-

ratories) to *Dag1* floxed mice (14). Expression of Cre-recombinase in nestin-Cre expressing cells, including neurogenic progenitors of the cerebrum, begins around E10.5 (25, 32). Breeders used to produce embryos and pups for these studies were male nestin-Cre⁺/*Dag1*^{L/L} and female *Dag1*^{L/L}. The DG null offspring were born in the expected Mendelian ratio. For timed pregnancy matings, noon of the day that the vaginal plug was observed was considered E0.5. Pregnant dams were injected with 40 mg/kg bromodeoxyuridine (BrdU) several days (migration studies) or 3 hours (proliferation studies) before death. Animal use procedures were approved by the University of Iowa Institutional Animal Care and Use Committee.

Antibodies

The following rabbit polyclonal antibodies were used: anti-laminin (1:1000) and anti- γ -aminobutyric acid (1:2000) from Sigma (St. Louis, MO); anti-Tbr1 (1:2500) and anti-Tbr2 (1:2000) from the laboratory of Robert F. Hevner (Seattle, WA); anti- β -DG (1:25) AP83 from the laboratory of Kevin P. Campbell (Iowa City, IA) (33); anti-Er81 (1:1500) from the laboratory of T. Jessell (New York, NY); anti-Ror β (1:2000) from the laboratory of Henk Stunnenberg (Nijmegen, Netherlands); anti-phosphohistone-H3 (1:400) from Upstate Biotechnology (Lake Placid, NY); anti-CDP (Cux1, 1:1000) from Santa Cruz Biotechnology (Santa Cruz, CA); anti-Dlx (1:75) from the laboratory of Jhumku D. Kohtz (Chicago, IL); and anti-Dab1 (1:400) from the laboratory of Jonathan Cooper (Seattle, WA).

Mouse monoclonal antibodies used were anti-reelin (1:1000) from Calbiochem (San Diego, CA); anti-neuronal-specific nuclear protein (NeuN, 1:1000), anti-proliferating cell nuclear antigen (PCNA, 1:2000), and anti-gial fibrillary acidic protein (GFAP, 1:1000) from Chemicon (Temecula, CA); anti- α -DG (1:400, clone I1H6C4) from Upstate Biotechnology; anti- β -DG (1:50, clone 7D11), anti-Pax6 (1:2000), RC2 (1:25, ascites), and anti-nestin (rat-401; 1:100) from Developmental Studies Hybridoma Bank (Iowa City, IA).

Rat monoclonal antibodies used were anti-BrdU (1:200) from Accurate (Westbury, NY) and anti-CTIP2 (1:1000) from Abcam (Cambridge, MA).

Immunohistochemistry

Brains were fixed in 4% paraformaldehyde with 4% sucrose in PBS and embedded in OCT. Coronal 12- μ m cryostat sections of the cerebral cortex were incubated for 30 minutes at room temperature in blocking solution (PBS containing 5% normal goat serum, 2% bovine serum albumin, and 1% Triton X). Sections were briefly boiled in 10 mmol/L sodium citrate (pH 6.0) up to 3 times for antigen retrieval and then incubated with primary antibodies overnight at 4°C followed by incubation with secondary antibodies (Alexa Fluor; Molecular Probes, Eugene, OR) at room temperature for 2 hours. Sections tested for BrdU staining were treated with 2N hydrogen chloride at 37°C for 30 minutes before sodium citrate boils. Sections were counterstained with 0.01% DAPI (Sigma) or TO-PRO-3 (Molecular Probes) to label nuclei.

TUNEL Analysis

Coronal, 12- μ m tissue sections were reacted using an in situ cell death detection kit (Roche, Indianapolis, IN), according

to the manufacturer's protocol except for the permeabilization step, which was previously shown not to affect sensitivity. Sections were counterstained with 4',6-diamidino-2-phenylindole (DAPI) to label nuclei.

In Situ Hybridization

A digoxigenin-labeled 1,182-bp mDag1 cDNA for riboprobes was subcloned from an mDag1 full-length cDNA clone (Accession No. BC007150) using Pst1 sites to excise cDNA spanning part of the 3' translated and untranslated regions. In situ hybridization was performed as previously described using 12- μ m coronal sections (34).

Retrograde Axon and RG Basal Process Tracing

Embryos and brains from postnatal mice were fixed by immersion in 4% paraformaldehyde in PBS with 4% sucrose. Brains were removed from the skull, dissected appropriately for the specific experiment, and then injected with the lipophilic carbocyanine tracer DiI (Invitrogen, Eugene, OR) and left to incubate in the dark at room temperature for 1 day to 10 weeks, depending on the specific experiment. Brains were then embedded in 4% agarose in PBS, and coronal 50- to 100- μ m sections were made on a vibratome. Some sections were incubated with primary and secondary antibodies and counterstained with DAPI and TO-PRO-3, as previously described.

Microscopy and Image Analysis

Sections were examined, and digital images were made by epifluorescence microscopy (Nikon E600), laser scanning confocal microscopy (Bio-Rad Radiance LS2000), bright field and Apotome epifluorescence microscopy (Zeiss Axioimager Z1, Jena, Germany). Color inversion of DiI labeling and contrast, sharpness, and brightness of images were enhanced using Adobe Photoshop CS2 (Adobe Systems, San Jose, CA). For in situ hybridization experiments with immunofluorescence, bright field images of mDag1 signal were pseudocolored using Adobe Photoshop CS2.

RESULTS

Dag1 Is Expressed by RG in the Embryonic VZ

Although the importance of DG in brain development has been confirmed in previous studies, the cell types in the embryonic cortex that express DG have not been well established. We examined *Dag1* mRNA expression during early (E12.5), middle (E14.5 and E15.5), and late (E18.5) neurogenesis. *Dag1* mRNA expression was low at E12.5 but was significantly higher at E15.5 and E18.5 (Figs. 1A–C). At all 3 time points, *Dag1* mRNA expression was restricted to the VZ, except for a small amount of expression in the cortical plate (CP) at E15.5 and E18.5 during the late stages of neurogenesis, consistent with data posted elsewhere (see Brain Gene Expression Map databank, Accession No. NM_010017, www.stjudebgem.org). *Dag1* mRNA colocalized in VZ cells with transcription factor Pax6, a marker of mainly RG (Fig. 1D). Pax6 is also expressed in some newly generated IPCs in the VZ (35, 36).

The protein product of *Dag1* is posttranslationally processed into α -DG and β -DG, 2 noncovalently linked subunits of the transmembrane dystrophin glycoprotein complex (37). Given the presumed role of DG in PBM-RG signaling, we examined the distribution of α -DG and β -DG in RG during neocortical histogenesis. The β -DG was localized to the end feet of RG basal processes at the outer surface of the neuroepithelium at the PBM and in association with meningeal and cortical blood vessels at E15.5 (Fig. 1E). The latter finding is most likely caused by DG expression by vascular endothelial cells or (at later ages) astrocytes (38). There was no detectable β -DG expression within the remaining extent of the cortex, including the VZ where *Dag1* mRNA was located (Fig. 1E). At P0.5, β -DG expression appeared as a thin line of immunoreactivity predominantly at the PBM (Figs. 1F, G). The β -DG expression colocalized with the terminal end feet of RG basal processes identified by antigen RC2 expression, where they attach to the PBM (Fig. 1H). Using high-magnification confocal microscopy, α -DG protein expression was likewise consistently found to be limited to the RG end feet–PBM interface throughout neurogenesis (as well as cerebral blood vessels) (Figs. 1I–L).

PBM-RG Interactions Mediated by DG Are Necessary for PBM Integrity

As expected, *Dag1* mRNA expression was undetectable in E12.5, E15.5, and E18.5 *Dag1* conditional knockout (cKO) brains because of conditional loss of *Dag1* expression by all nestin-expressing cells beginning at E10.5, including Pax6-positive RG in the neocortex (Figs. 1M–O). The β -DG protein was present in association with meningeal blood vessels but was completely absent from RG basal processes by E18.5 (Figs. 1Q–T). In *Dag1* cKO brains, α -DG protein immunoreactivity was similar to that observed in *Dag1*^{+/+} mice at E12.5, likely reflecting earlier expression of *Dag1* by RG (or neuroepithelial cells) before the onset of nestin-Cre expression at about E10.5 but weakened throughout the neurogenic period and was completely absent from the RG-PBM interface by E18.5 (Figs. 1U–X). After a temporal pattern similar to the loss of DG protein from RG end feet, the PBM developed gaps and became increasingly disrupted in *Dag1* cKO brains (Figs. 1U–X).

To investigate the effects of DG loss on RG basal process morphology and attachment to the PBM, we injected P0.5 *Dag1*^{+/+} and *Dag1* cKO cortical VZs with the lipophilic carbocyanine dye DiI. Immunoreactivity for nestin and for RC2, an intermediate filament-associated protein expressed only in RG, was also used to examine basal process morphology (39). All DiI-, nestin- (data not shown), and RC2-labeled RG basal processes in P0.5 *Dag1*^{+/+} brains terminated on intact PBM (Figs. 2A, C). In contrast, despite PBM disruptions at P0.5, RG basal processes in *Dag1* cKO brains remained attached to residual islands of PBM (Figs. 2B, D). However, even in areas where RG-PBM attachment persisted at P0.5, RG basal processes lost the orderly, parallel, radial arrangement that was characteristic of basal processes in *Dag1*^{+/+} brains and instead became severely disorganized (Figs. 2B, D). Furthermore, some RG basal processes extended beyond the original PBM into the meninges and often attached to ectopic fragments of PBM, thus

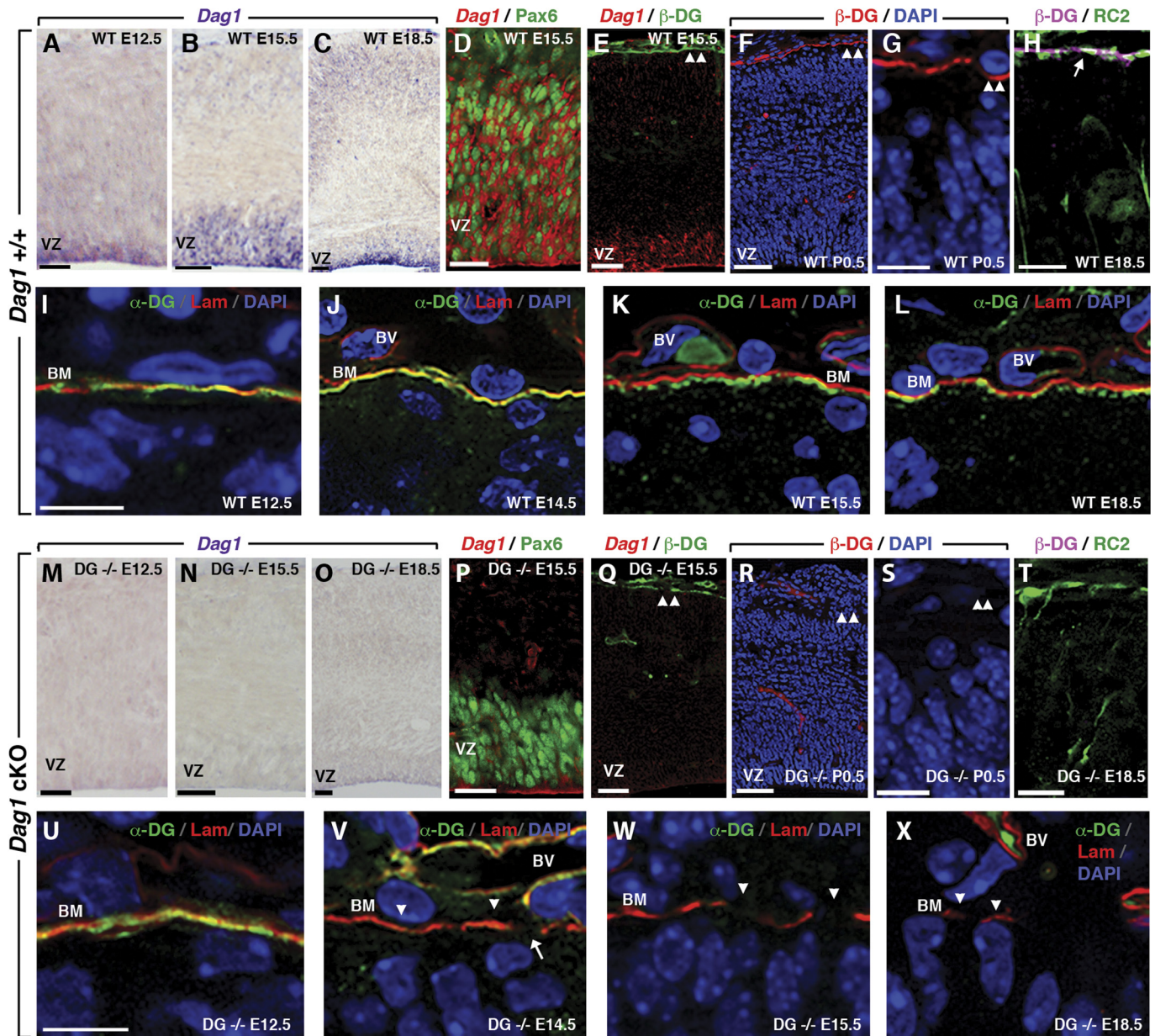
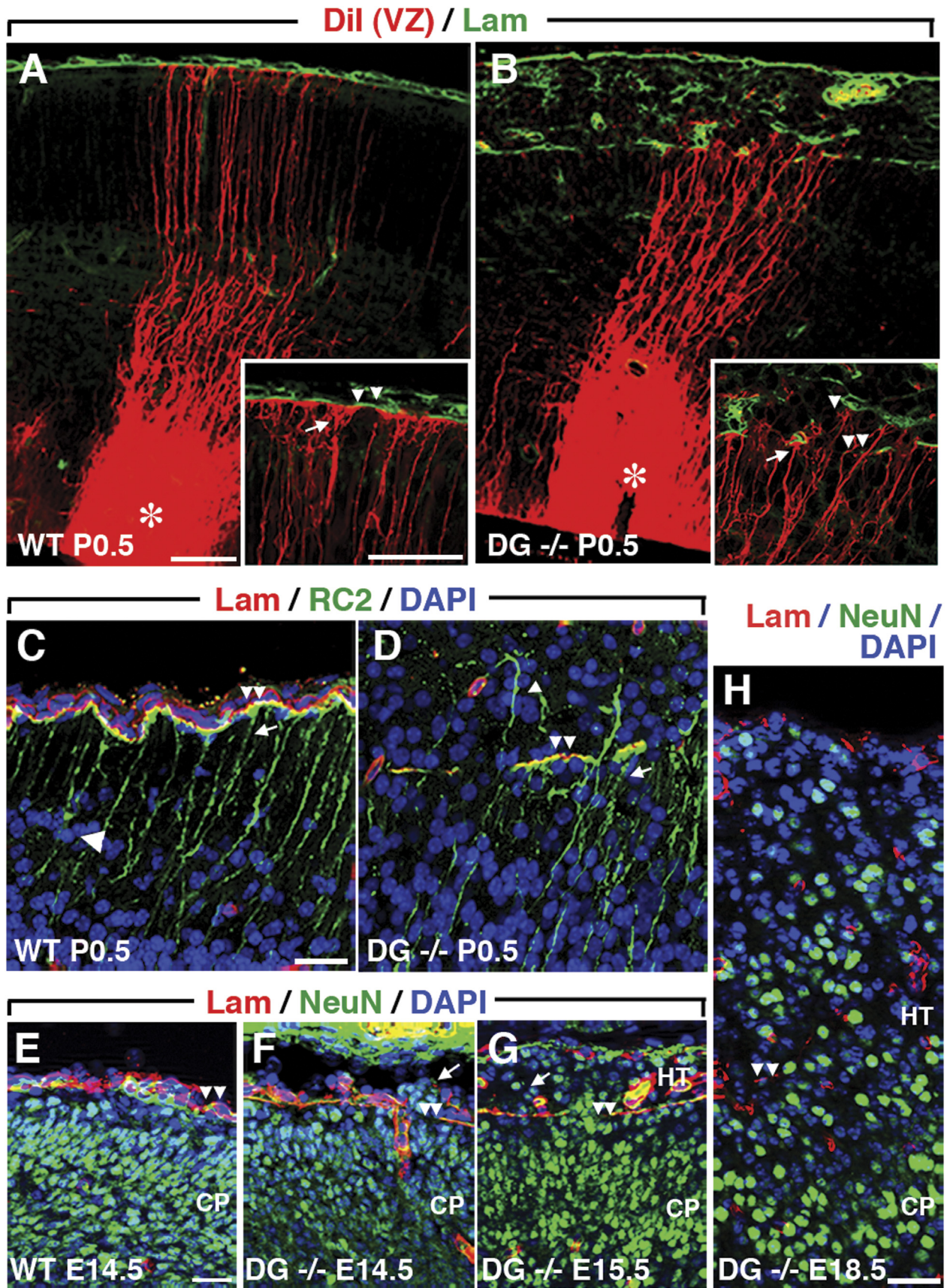


FIGURE 1. Dystroglycan is expressed by RG during neurogenesis. In *Dag1*^{+/+} (wild-type [WT]) brains, *Dag1* mRNA expression is weak and restricted to the VZ at E12.5 (A) and E15.5 (B) and is mostly in the VZ but also sporadically in CP cells at E18.5 (C). *Dag1* mRNA is expressed in Pax6-positive RG soma in the VZ at E15.5 (D, E) but not at the PBM where β-DG protein is expressed (E, arrowheads). The β-DG is restricted to the glia limitans at the outermost aspect of the basal cortex at P0.5 (F, arrowheads; higher magnification in G). At E18.5, β-DG colocalizes with RC2-positive RG end feet (H, arrow). Using high-magnification confocal microscopy, α-DG protein consistently colocalizes with the laminin-positive BM at E12.5 (I), E14.5 (J), E15.5 (K), and E18.5 (L). (M–X) In *Dag1* cKO (*DG*^{-/-}) brains, *Dag1* mRNA is absent at E12.5 (M), E15.5 (N), and E18.5 (O) and is not expressed in Pax6-positive RG soma (P). The β-DG protein expression is irregular at E15.5 (Q, arrowheads) and absent at P0.5 (R, higher magnification in S). At E18.5, β-DG is not expressed in RC2-positive RG end feet (T, arrow). The α-DG colocalizes with the BM at E12.5 (U). By E14.5, α-DG is nearly absent, whereas the BM remains mostly intact (arrowheads) with only small disruptions (arrow) (V). The α-DG is entirely absent, and there is widespread disruption of the BM at E15.5 (W, arrowheads). At E18.5, only small fragments of the BM remain (X, arrowheads). BV, blood vessel; WT, *Dag1*^{+/+}; *DG*^{-/-}, *Dag1* cKO. Scale bars = (A, C, D, M, O, P) 25 μm; (B, E, F, N, Q, R) 50 μm; (G–L, S–X) 12.5 μm.

contributing to the formation of leptomenigeal heterotopia (Fig. 2B, inset). In addition, many NeuN-positive neurons were closely associated with RG basal processes below layer I in the CP of *Dag1*^{+/+} brains (Fig. 2C, single arrowhead),

consistent with the normal migration of newborn pyramidal neurons along RG fibers during cortical histogenesis (40, 41). Neurons were similarly associated with RG fibers of *Dag1* cKO brains; this association persisted ectopically into layer I



(the marginal zone [MZ]) and the leptomeninges (Fig. 2D, single arrowhead).

PBM Disintegration Provides a Permissive Environment for Neuronal Overmigration

Intact PBM in *Dag1*^{+/+} brains smoothly delimited the brain surface and established the glia limitans below which CP neurons remained throughout embryogenesis (Fig. 2E). However, where breaches of the PBM arose in *Dag1* cKO brains, there were ectopic clusters of neurons (heterotopia) in the meninges as early as E14.5 (Fig. 2F). As PBM defects became more widespread at E15.5 and most of the PBM was lost by E18.5, greater numbers of ectopic neurons accumulated beyond the glia limitans, resulting in a supracortical layer of neural tissue that was confluent with the underlying residual cortex (Figs. 2G, H). Displaced neurons and glia in intracerebral (e.g. periventricular), intracranial but extracerebral (e.g. meningeal), or extracranial locations (e.g. pulmonary) may be associated with various familial and spontaneous cerebral malformation disorders or fetal alcohol syndrome because of abnormal neuronal migration or as tumors in humans and laboratory rodents and are referred to as either neuroglial ectopia or heterotopia (6, 14, 42–47). Hereafter, we will refer to the supracortical accumulation of neurons and glia in *Dag1* cKO brains as “leptomeningeal heterotopia” and displaced neurons or glia as “heterotopic” if they are within the leptomeninges or “ectopic” if they are in any abnormal location.

Proliferation of Heterotopic Progenitor Cells

Cerebrocortical pyramidal neurons are produced by 2 main types of progenitor cells, RG and IPCs, which are derived from RG (36). Radial glia express transcription factor Pax6 and are restricted to the VZ (31). Intermediate progenitor cells are produced by RG in the VZ, migrate into the SVZ, and express transcription factor Tbr2 (36). We classified RG or IPCs as ectopic if Pax6-positive nuclei or Tbr2-positive nuclei, respectively, were superficial to the cortical subplate. The subplate was defined as the lamina of the dorsal cortex immediately apical to the cell-dense CP (layer VI) and basal to the cell-sparse intermediate zone (IZ). At E14.5, when only small and infrequent disruptions of the PBM were present in *Dag1* cKO brains, few ectopic RG or IPCs were observed in cortical slices of either *Dag1* cKO brains or *Dag1*^{+/+} brains and there was no apparent difference in VZ thickness between these genotypes (Figs. 3E–G).

Ectopic Pax6-positive radial glia, Tbr2-positive IPCs, and Pax6-positive/Tbr2-positive cells (newly generated IPCs), located mostly in meningeal heterotopia, were common in E15.5 and E18.5 *Dag1* cKO brains but were very rare in E15.5 and E18.5 wild-type brains (Figs. 3A–C, E, F). Ectopic progenitor cells were present as single cells or in mixed clusters and varied widely in total numbers among different *Dag1* cKO brains (Figs. 3B, C, E, F). No ectopic Pax6-positive cells in P0.5 *Dag1* cKO brains expressed the astrocytic marker GFAP, but there were small clusters of GFAP-positive Pax6-astrocytic cells detected in meningeal heterotopia of P0.5 *Dag1* cKO brains, consistent with previous findings (Fig. 3D) (14).

The VZ of E15.5 and E18.5 *Dag1* cKO brains was slightly thinner than that in *Dag1*^{+/+} brains, which may have been a result of RG overmigration from the VZ to ectopic locations or, possibly, apoptosis of RG in the VZ (Figs. 3A, B, G). Using the terminal deoxynucleotidyl transferase dUTP nick end labeling (TUNEL) method, we detected no increase of apoptotic cells in the VZ of E14.5, E15.5, or E18.5 *Dag1* cKO brains (data not shown). At P0.5, the number of ectopic RG and IPCs in *Dag1* cKO brains declined relative to E15.5 and E18.5 (Figs. 3E, F). This may have been a result of terminal differentiation of ectopic progenitors and reduced migration of additional progenitors from the VZ and SVZ; apoptosis of ectopic progenitors may have contributed to this decline as well because rare (1–3 per 12- μ m coronal section) apoptotic cells were seen in P0.5 *Dag1* cKO heterotopia or CPs (data not shown).

Using multiple markers of mitotically active cells, including expression of the phosphorylated form of histone-H3 (PHH3), chromatin condensation, acute BrdU incorporation, and expression of PCNA, we investigated whether ectopic RG and IPCs in *Dag1* cKO brains were mitotically active despite being located outside their normal progenitor niches (VZ and SVZ) (48, 49). In E15.5 and E18.5 *Dag1* cKO brains, frequent ectopic RG and IPCs in the CP and heterotopia had condensed chromatin (mitotic figures) and expressed PH3, a marker of proliferating cells in G2 or M phase of the cell cycle (Figs. 3H–O). Ectopic Pax6/Tbr2 double labeled cells, representing newly differentiating IPCs (36), were also relatively frequent in E15.5 and E18.5 *Dag1* cKO brains (Figs. 3D, arrow). These cells often showed mitotic chromatin (Figs. 3P–S). Many ectopic RG and IPCs were labeled with BrdU, a thymidine analog incorporated into DNA during the S phase, after pregnant dams were injected 3 hours before killing (Figs. 3T, U). In E15.5 *Dag1* cKO brains, nearly one half of ectopic RG (15 of

FIGURE 2. Basement membrane disintegration leads to RG fiber abnormalities and heterotopia (HT). **(A)** In a wild-type (WT) *Dag1*^{+/+} brain, RG fibers (arrows) extend to the BM (arrowheads) (higher magnification inset). **(B)** In a *Dag1* cKO brain, RG fibers attach to intact areas of the BM (arrow) and frequently extend into meningeal spaces through breaches in the BM (double arrowheads) where some fibers remain attached to ectopic BM (single arrowhead) (higher magnification in inset). **(C)** RC2-positive RG basal processes (arrow) terminate at the BM (arrowheads), and most neurons (single arrowhead) are closely associated with RG fibers in a P0.5 *Dag1*^{+/+} brain. **(D)** In a *Dag1* cKO brain, some RG fibers (arrow) attach to intact BM (double arrowheads), whereas other RG fibers with closely associated neurons (single arrowhead) extend into the meninges (MG) through gaps in the BM. **(E)** The distribution of NeuN-positive cortical neurons is smoothly delimited at the glia limitans to the neuroepithelium by intact BM (arrowheads) in an E14.5 *Dag1*^{+/+} brain. **(F)** Small neuronal HT (arrows) are present directly above gaps in the BM (arrowheads) in an E14.5 *Dag1* cKO brain. **(G, H)** Greater numbers of cortical neurons (arrow) are present in meningeal spaces above intact and disrupted (arrowheads) BM in a *Dag1* cKO E15.5 brain **(G)**, and by E18.5, the HT are large and confluent with small underlying remnants of BM (arrowheads) **(H)**. Scale bars = **(A, B)** 50 μ m; **(A, B insets)** 50 μ m; **(C, D)** 25 μ m; **(E–H)** 100 μ m.

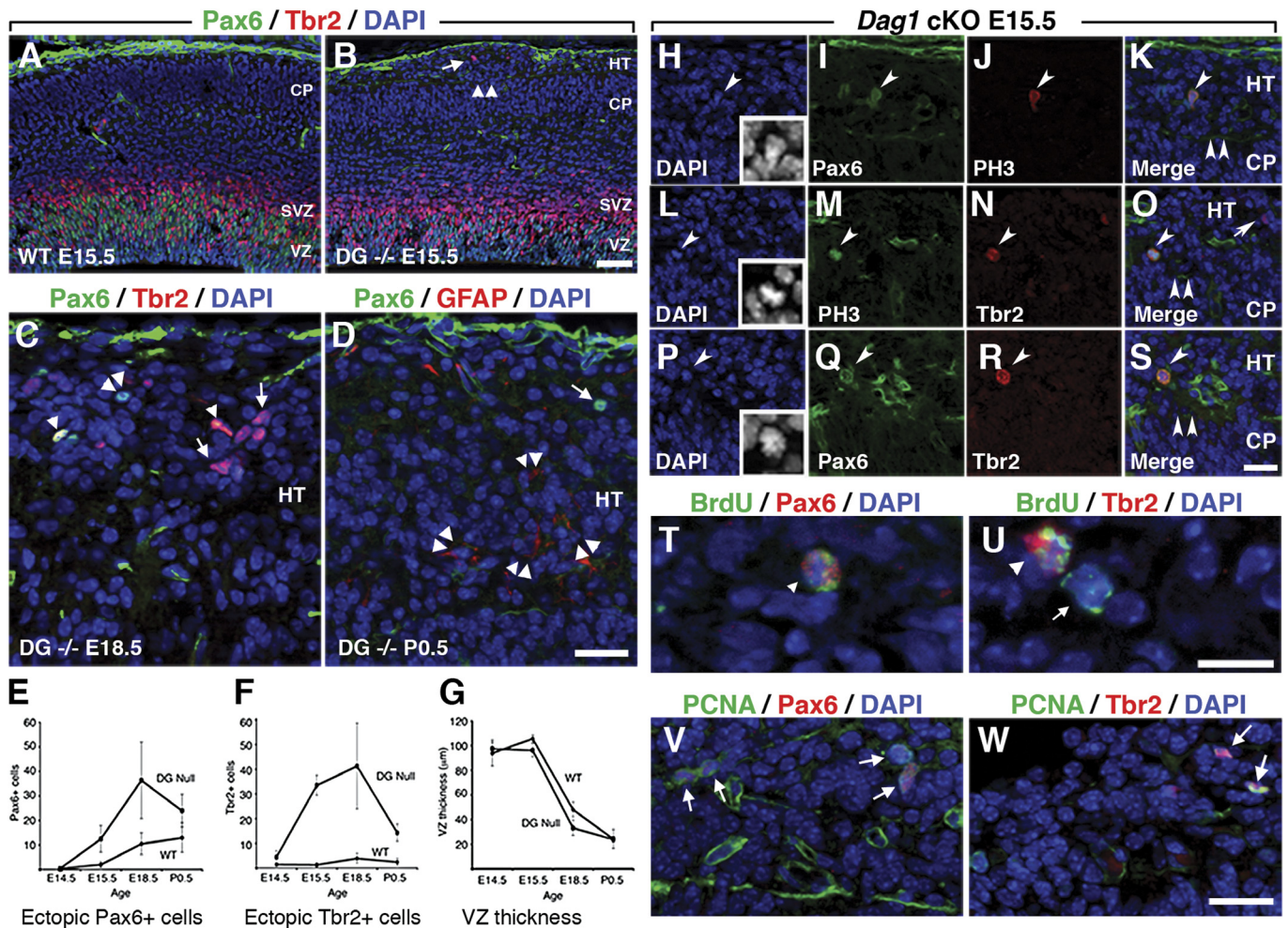


FIGURE 3. Ectopic proliferating progenitor cells in the CP and heterotopia (HT) of *Dag1* cKO brains. (**A–G**) As expected, Pax6-positive RG and Tbr2-positive IPCs are in the VZ and SVZ, respectively, of E15.5 wild-type and *Dag1*^{+/+} and *Dag1* cKO (DG^{-/-}) brains (**A, B**). There are, however, frequent ectopic Pax6-positive RG (**C**, double arrowheads), Tbr2-positive IPCs (**B, C**, single arrow), and recently born Pax6-positive/Tbr2-positive IPCs (**C**, single arrowhead) that are present singly (**B**) and in large clusters (**C**) in the CP and HT above disrupted BM (**B**, double arrowheads) of E15.5, E18.5, and P0.5 *Dag1* cKO brains (**B, C, E, F**). The VZ of *Dag1* cKO brains (**B, G**) frequently seems slightly thinner than *Dag1*^{+/+} brains (**A, G**) at E15.5 and E18.5 but not at E14.5 or P0.5 (**A, B, G**). At P0.5, clusters of GFAP-positive astrocytes (double arrowheads) are present in heterotopia, whereas heterotopic Pax6-positive RG (arrow) are GFAP negative (**D**). (**H–W**) In E15.5 *Dag1* cKO brains, heterotopic RG (**I, K**, single arrowhead), IPCs (**N, O**, single arrowhead), and heterotopic Pax6-positive/Tbr2-positive recently born IPCs (**Q, R, S**, single arrow and arrowhead) are present above disrupted BM (**K, O, S**, double arrowheads) and frequently have condensed chromatin (mitotic figures) (**H, L, P**, arrowhead, and inset) and express PH3 (**J, K, M, O**, single arrowhead). Heterotopic RG (**T**, arrowhead), Tbr2-positive IPCs (**U**, arrowhead), and Tbr2- heterotopic cells (**U**, arrow) are acutely labeled with BrdU in E15.5 *Dag1* cKO brains. Many heterotopic RG (**V**, arrows) and most heterotopic IPCs (**W**, arrows) express PCNA in E15.5 *Dag1* cKO brains. Scale bars = (**A, B**) 50 µm; (**C, D, H–S, V, W**) 25 µm; (**T, U**) 12.5 µm. Y axis, average cell number/coronal section; X axis, time point (**E, F**). Y axis, average VZ thickness (µm); X axis, time point (**G**).

33, 45%) and two thirds of ectopic IPCs (18 of 28, 64%) expressed PCNA (Figs. 3V, W).

Marked Dyslamination and Heterotopic Distribution of Diverse Cortical Neurons

We used layer- and subtype-specific mRNA and protein expression of CP neurons to investigate the pathogenesis of dyslamination and heterotopia formation in *Dag1* cKO brains (50). At completion of migration, CR cells normally reside in

the embryonic MZ (postnatal layer I) immediately below the PBM where they produce and secrete reelin, a glycopeptide that is essential for proper lamination of radially migrating neurons (51, 52). In E14.5, E16.5, and P0.5 *Dag1*^{+/+} brains, CR cells were mostly horizontally oriented in a monolayer within the cell-sparse MZ (Figs. 4A, C, E). Between E14.5, E16.5, and P0.5 in *Dag1* cKO brains, increasing numbers of CR cells accumulated in meningeal heterotopia above gaps in the CR cell monolayer in the MZ (Figs. 4B, D, F, G). Deep to

these CR cell layer gaps, the laminar pattern of the CP was disrupted, and columns of cells extended through the gaps into heterotopia (Figs. 4D). Individual ectopic CR cells were scattered individually or in small numbers throughout meningeal heterotopia, but occasionally they formed clusters or, remarkably, formed monolayers along the outermost aspect of the meningeal heterotopia that resembled layer I of normal CPs (Figs. 4F, G).

In both *Dag1*^{+/+} and *Dag1* cKO brains, cells immunoreactive for CTIP2, a transcription factor expressed in early-

born subcerebral projection neurons, were present in layer V at E14.5, E15.5, and E18.5 (Figs. 4H–M) (53). However, in *Dag1* cKO brains only, CTIP2-positive cells were also present in more superficial CP layers and in meningeal heterotopia, with a concurrent reduction of CTIP2-positive cells in layer V (Figs. 4I, K, M). Projection neurons and CR cells expressing Tbr1, a T-box transcription factor, were present in the subplate, layer VI, and the MZ of E14.5, E15.5, and E18.5 *Dag1*^{+/+} and *Dag1* cKO brains (Figs. 5A–F) (54). In *Dag1* cKO brains, Tbr1-positive cells were also present in meningeal heterotopia

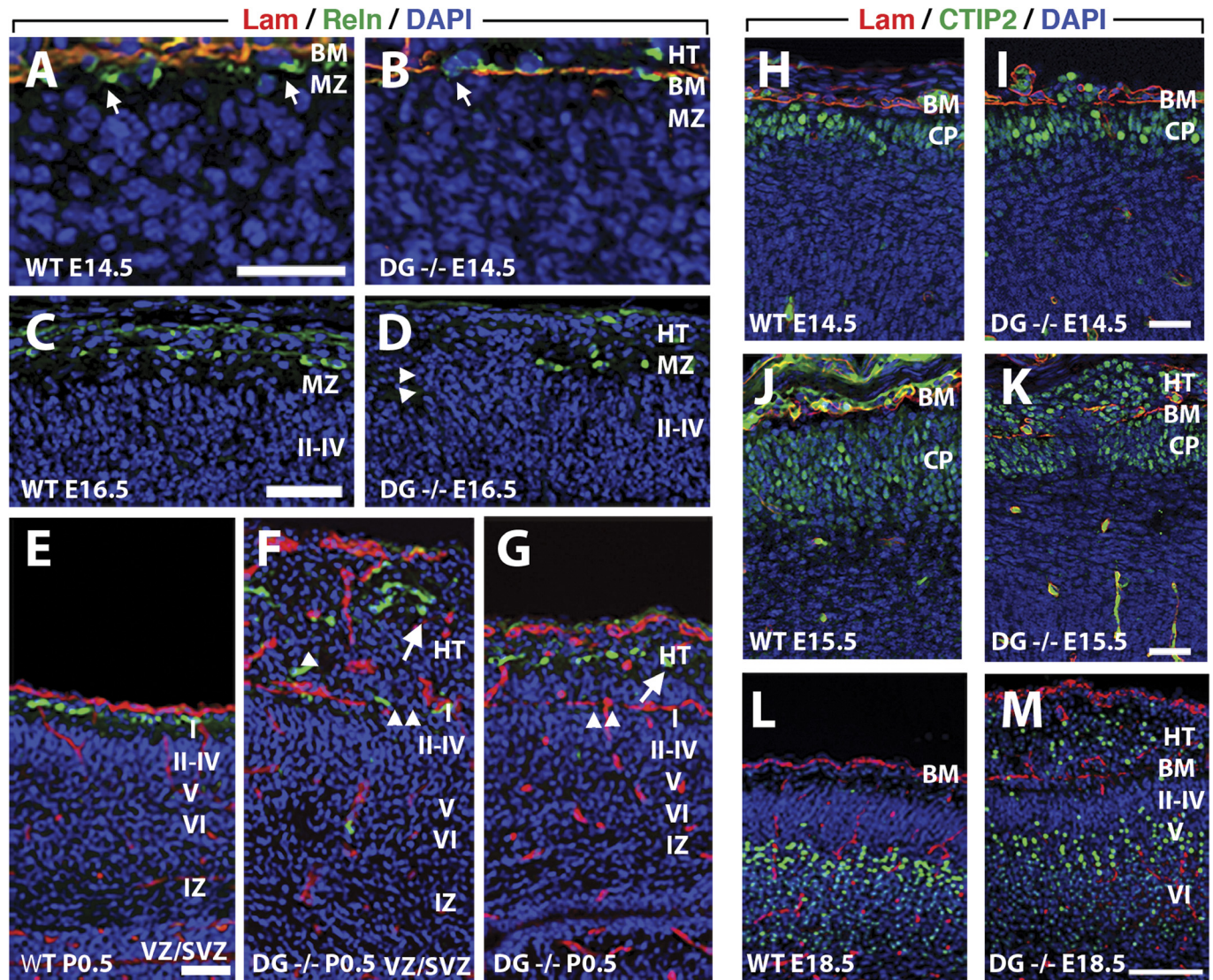


FIGURE 4. Cajal-Retzius cells and CTIP2-positive layer V neurons migrate through early BM breaches into meningeal spaces. **(A–G)** Reelin-positive CR cells form a monolayer in the marginal zone (MZ, layer I) directly below intact pial BM in wild-type (*WT*) *Dag1*^{+/+} E14.5 **(A)**, arrows), E16.5 **(C)**, and P0.5 **(E)** brains. The CR cells **(B)**, arrow) migrate through small BM gaps in E14.5 *Dag1* cKO (*DG*^{-/-}), brains. In E16.5 *Dag1* cKO brains, many CP neurons migrate into meningeal heterotopia (HT) through large gaps (double arrowheads) in the CR cell layer **(D)**. At P0.5, most CR cells are in meningeal HT above disrupted BM **(F, G)**, double arrowheads) and are arranged randomly **(F)**, single arrowhead) in clusters **(F)**, single arrow) and less frequently in single layers **(G)**, single arrow), resembling layer I of *WT* CPs. **(H–M)** Intact BM overlays layer V CTIP2-positive neurons in *Dag1*^{+/+} brains at E14.5 **(H)**, E15.5 **(J)**, and E18.5 **(L)**. Between E14.5 **(I)**, E15.5 **(K)**, and E18.5 **(M)**, CTIP2-positive neurons progressively accumulate in superficial CP layers and meningeal heterotopia of *Dag1* cKO brains above disrupted BM. Scale bars = **(A, B, E–K)** 25 μ m; **(C, D)** 50 μ m; **(L, M)** 100 μ m.

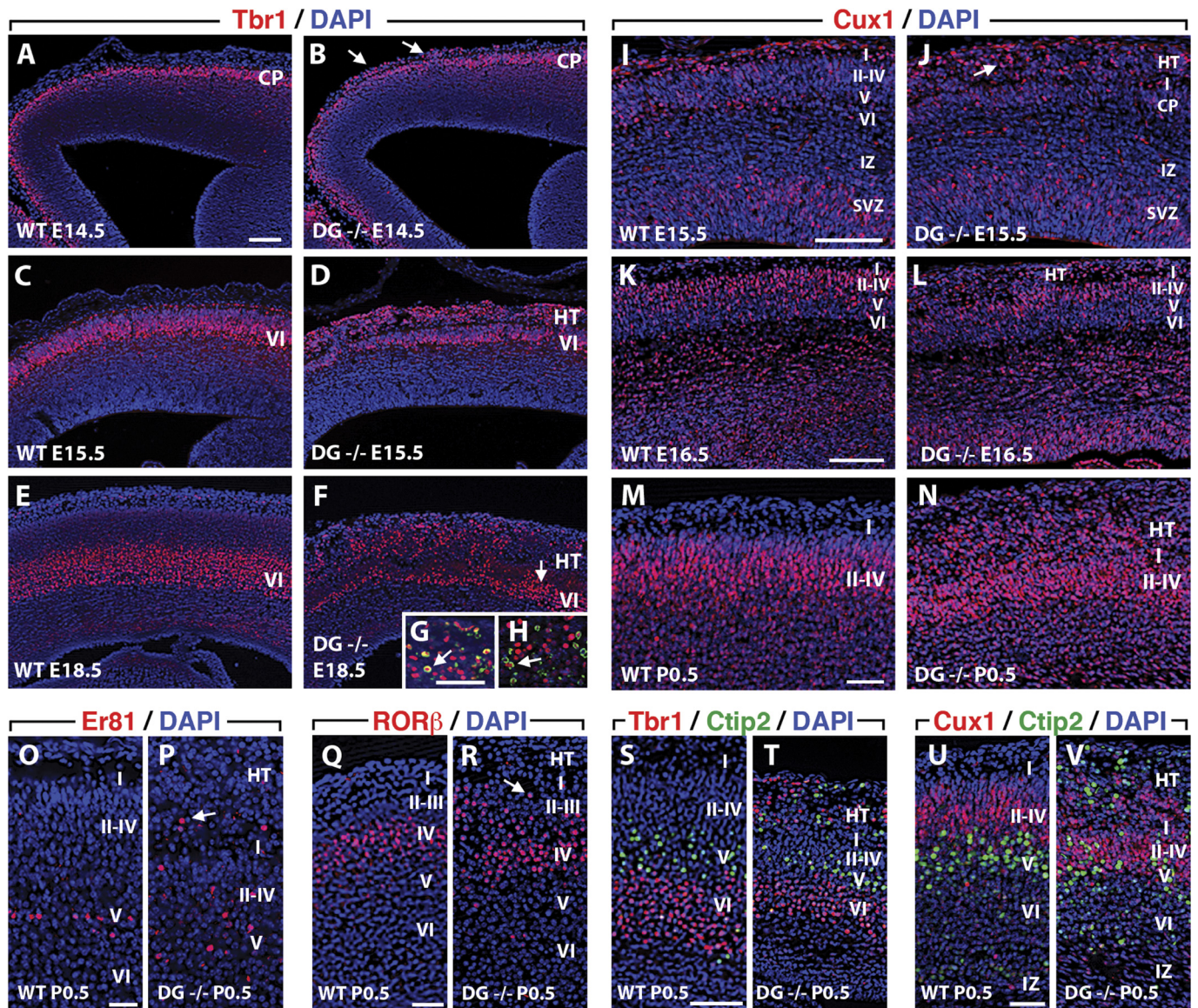


FIGURE 5. Marked dyslamination and expansion of heterotopia (HT) during late neurogenesis are associated with overmigration of deep and superficial CP neurons. **(A–H)** The Tbr1-positive CP layer VI in *Dag1*^{+/+} brains progressively expands between E14.5 **(A)**, E15.5 **(C)**, and E18.5 **(E)**. In addition to CP layer VI, small numbers of heterotopic Tbr1-positive neurons are present in *Dag1* cKO (*Dag1*^{-/-}) E14.5 brains **(B)**, arrows). Many more heterotopic Tbr1-positive neurons are present at E15.5 **(D)** compared with E14.5 **(B)**, and the thickness of Tbr1-positive cells in layer VI **(D)** seems much reduced at E15.5 in *Dag1* cKO brains compared with wild-type (WT) *Dag1*^{+/+} brains **(C)**. Despite substantial expansion of meningeal HT, few additional heterotopic Tbr1-positive neurons are present in *Dag1* cKO E18.5 brains **(F)** compared with E15.5 brains **(D)**, and many areas in layer VI still have large numbers of appropriately laminated Tbr1-positive cells at E18.5 **(F)**, arrow). **(I–N)** Many early-born Tbr1-positive/BrdU-positive (E12.5) neurons (arrow) are present in *Dag1* cKO P0.5 HT despite birth dates several days before BM disruption **(G)**, HT). Although occasional late-born Tbr1-positive/BrdU-positive (E15.5) neurons (arrow) are present in *Dag1* cKO P0.5 HT, many late-born Tbr1-positive neurons are appropriately laminated in CP layer VI despite BM disruption before their birth and migration **(H)**, layer VI). **(I–N)** Many late-born Cux1-positive neurons are present in layers II to IV in *Dag1*^{+/+} brains at E15.5 **(I)**, E16.5 **(K)**, and P0.5 **(M)**. Small numbers of heterotopic Cux1-positive neurons are present in *Dag1* cKO E15.5 brains **(J)**, arrows), whereas slightly more and substantially more are present at E16.5 **(L)** and P0.5 **(N)**, respectively. Despite widespread BM disruption before their birth and migration through the CP, many Cux1-positive neurons are appropriately laminated in layers II to IV at P0.5 **(N)**. **(O, P)** Er81-positive neurons are restricted to the deep aspect of layer V in P0.5 *Dag1*^{+/+} brains **(O)** but are present in layers I to V and heterotopia (arrow) in *Dag1* cKO brains **(P)**. **(Q, R)** Rorβ-positive neurons are only present in layer IV in P0.5 *Dag1*^{+/+} brains **(Q)** but are distributed throughout layers I to IV (arrow) in *Dag1* cKO brains **(R)**. **(S, T)** CTIP2-positive neurons are mostly limited to layer V and are superficial to earlier born Tbr1-positive neurons in layer VI in P0.5 *Dag1*^{+/+} brains **(S)** but Tbr1-positive neurons are also admixed with CTIP2-positive neurons in layers I to V and heterotopia in *Dag1* cKO brains **(T)**. **(U, V)** Cux1-positive neurons in layers II to IV are superficial to earlier born CTIP2-positive neurons in layer V in *Dag1*^{+/+} brains **(U)** but are also admixed with Cux1-positive cells in layers I to IV and HT in *Dag1* cKO brains **(V)**. Scale bars = **(A–F)** 200 μm; **(I–N)** 100 μm; **(G, H, O–V)** 50 μm.

overlying areas of the CP with substantial thinning of layer VI (Fig. 5B). The numbers of heterotopic Tbr1-positive cells and CTIP2-positive cells increased significantly in *Dag1* cKO brains between E14.5 and E18.5, especially from E14.5 to E15.5 (Figs. 4I, K, M; 5B, D, F). Tbr1-positive cells and CTIP2-positive cells, with birth dates between E11.5 and E15.5 (55), were born both before and after significant disruption of the PBM in *Dag1* cKO brains. Many E12.5 (Fig. 5G) and occasional E15.5 (Figs. 5H) BrdU-labeled Tbr1-positive cells were present in the heterotopia of P0.5 *Dag1* cKO brains, suggesting that projection neurons born before and after PBM breakdown migrated into meningeal heterotopia.

Most superficial layer neurons, including layer II to IV cells, had birth dates between E13.5 and E16.5 (55) and, therefore, were born and migrated into the CP after significant disruption of the PBM had occurred in *Dag1* cKO brains. In E15.5, E16.5, and P0.5 *Dag1*^{+/+} and *Dag1* cKO brains, cells expressing the transcription factor Cux1 were present in layers II to IV (Figs. 5I–N). Cux1-positive cells also accumulated in meningeal heterotopia of *Dag1* cKO brains, particularly between E16.5 and P0.5, despite reduced heterotopic migration of early-born neurons (CTIP2 positive and Tbr1 positive) during this period (Figs. 5J, L, N).

Individual CP layers contain multiple subtypes of projection neurons, and at the same time, specific projection neuron subtypes may normally be present in single or multiple CP layers (55). For example, Er81-positive cells include all layer V subcerebral and many layer V corticocortical projection neurons, whereas CTIP2-positive expression is limited to layer V subcerebral projection neurons (56, 57). In addition, Rorβ expression is restricted to layer IV neurons, whereas Cux1 is expressed by neurons in layers II to IV (58, 59). We investigated dyslamination of different neuronal subtypes in *Dag1* cKO brains that normally have similar or overlapping laminar fates but unique molecular expression patterns. We compared the distribution of neurons defined by either Er81-positive or Rorβ-positive expression to that of CTIP2-positive and Cux1-positive neurons, respectively. In P0.5 *Dag1*^{+/+} brains, Er81-positive neurons were in the deep (apical) aspect of layer V (Fig. 5O) but in *Dag1* cKO brains, few Er81-positive neurons laminated appropriately in layer V and most were in layers I to IV and heterotopia (Fig. 5P). Interestingly, fewer Er81-positive neurons laminated appropriately in *Dag1* cKO brains compared with other layer V neuronal subtype CTIP2-positive cells (Fig. 4M). All Rorβ-positive neurons in P0.5 *Dag1*^{+/+} brains were in layer IV (Fig. 5Q). Although most Rorβ-positive neurons laminated appropriately in layer IV of P0.5 *Dag1* cKO brains, they were also frequently present in layers I to III (Fig. 5R) and heterotopia (data not shown) in a comparable pattern to Cux1-positive cells, which are likewise late-born neurons.

In normal CP development, deeper layers form before and beneath more superficial layers in an inside-out pattern based on birth date and molecular phenotype (55, 60, 61). In P0.5 *Dag1*^{+/+} brains, CTIP2-positive cells in layer V were above Tbr1-positive cells in layer VI with little overlap (Fig. 5S). In contrast, Tbr1-positive cells were mixed with CTIP2-positive cells in layer V, and both Tbr1-positive and CTIP2-positive cells were present in more superficial CP layers and meningeal heterotopia in P0.5 *Dag1* cKO brains (Fig. 5T).

Similarly, Cux1-positive cells in layers II to IV were above layer V CTIP2-positive cells in *Dag1*^{+/+} brains (Fig. 5U), but both were admixed in superficial CP layers and meningeal heterotopia without respect to normal laminar pattern in P0.5 *Dag1* cKO brains (Fig. 5V). Nevertheless, despite the large number of neurons from each of the CP layers that aberrantly migrated in *Dag1* cKO brains, there was a surprising degree of appropriate lamination within the mutant CP, and only rarely were CP projection neurons present in deeper than normal laminae of the cortex for their specific molecular expression phenotype (Figs. 5B, D, F, J, L, N, P, R, T, V). In this regard, neuronal “overmigration” accurately depicts this aspect of the *Dag1* cKO cortical phenotype.

Unlike projection neurons, interneurons are produced in the ventral telencephalon and migrate tangentially into the dorsal telencephalon through the MZ, IZ, and SVZ before migrating radially to establish laminar positions alongside projection neurons of similar birth dates (62–67). Dlx transcription factors are specifically expressed by cortical interneurons during the embryonic and postnatal periods (63). In E15.5 *Dag1*^{+/+} and *Dag1* cKO cortex, Dlx-positive interneurons similarly migrated in streams from the ventral telencephalon to the CP in tangential migratory streams from the ganglionic eminences (Figs. 6A, B). Within the dorsal cortex, most Dlx-positive interneurons were widely distributed among cortical layers, with greatest abundance in the IZ, SVZ, and (admixed with CR cells) in the MZ. In *Dag1* cKO cortex, some Dlx-positive cells also migrated into meningeal heterotopia (Fig. 6C, D). In E18.5 *Dag1*^{+/+} lateral neocortex, many Dlx-positive interneurons were still migrating to the dorsal telencephalon through the MZ, IZ, and SVZ, and some interneurons accumulated in layer V (Fig. 6E). In contrast, many Dlx-positive interneurons in E18.5 *Dag1* cKO lateral cortex were located not only in these zones but also in heterotopia overlying gaps in the MZ monolayer of reelin-positive CR cells (Figs. 6F). Compared with E15.5 brains, many more Dlx-positive interneurons had migrated into the dorsal cortex and were in layers I, V, and VI, VZ, and SVZ in both *Dag1*^{+/+} and *Dag1* cKO brains (Figs. 6G, H). Dlx-positive interneurons were also in the heterotopia of P0.5 *Dag1* cKO brains (Figs. 6H). Accumulation of Dlx-positive interneurons within meningeal heterotopia throughout the neurogenic period is consistent with the hypothesis that interneurons migrate to similar locations during the same period as projection neurons with the same birth dates and therefore are similarly susceptible to conditions that facilitate overmigration (67).

Heterotopic Pyramidal Neurons Establish Appropriate Axonal Projections

We used retrograde axon tracing with DiI to investigate cortical pyramidal neuron morphology and efferent axonal projections. As expected, DiI injections into the thalamic ventroposterior lateral nucleus resulted in retrograde labeling of corticothalamic neurons with somata in layer VI of the somatosensory cortex in both *Dag1*^{+/+} and *Dag1* cKO P7.5 brains (Figs. 7A, B); however, ectopic neurons in superficial CP layers and meningeal heterotopia of *Dag1* cKO brains also established connections with the ventroposterior lateral nucleus (Fig. 7B). DiI injections into the corpus callosum labeled neurons in all

layers of P7.5 *Dag1*^{+/+} and *Dag1* cKO brains, with the greatest abundance of callosal neurons in upper layers II to IV (Figs. 7C, D). Many neurons in *Dag1* cKO meningeal heterotopia also made callosal projections (Figs. 7D). Dil injections into the cerebral peduncles of P7.5 *Dag1*^{+/+} and *Dag1* cKO

brains retrogradely labeled neurons in layer V, but in addition, many neurons in *Dag1* cKO heterotopia were labeled from these injections (Figs. 7E–I). In P7.5 *Dag1*^{+/+} brains, pyramidal neurons had parallel arrangement of apical dendrites that terminated with tufts in layer I (Figs. 7A, E, G). The dendrites of heterotopic subcerebral projection neurons in P7.5 *Dag1* cKO brains were frequently oriented abnormally, with tortuous apical dendrites. In some cases, apical dendrites ran parallel to the surface of the heterotopia (Figs. 7H) or projected downward (toward the ventricle) and therefore opposite to the normal orientation of apical dendrites (Figs. 7I).

DISCUSSION

The complex process of neocortical development involves proliferation of progenitor cells in the dorsal and ventral telencephalon, long-distance migration of postmitotic neurons from progenitor zones into the CP, lamination of neurons according to birth date and molecular phenotype, and establishment of connections with cortical and subcortical targets (54, 60, 62, 68–70). Because PBM-RG signaling interactions are mediated by DG and have been shown to be essential for normal morphogenesis of the cerebral cortex, we investigated the expression of DG protein and *Dag1* mRNA in the developing neocortex. We used *Dag1* cKO brains to investigate which aspects of normal neocortical development are affected by disrupted PBM-RG interactions and the pathogenesis of cobblestone lissencephaly. We found that the disruption of PBM-RG interactions caused by *Dag1* mutation caused perturbations that altered the distribution and migration of progenitors and neurons but had little effect on the layer-specific (molecular) differentiation of pyramidal and nonpyramidal neuron types or on axon growth and targeting to thalamus, contralateral cortex, and cerebral peduncles. Our data provide a more complete understanding of the pathogenesis underlying cobblestone lissencephaly in some of the dystroglycanopathies. Key features of this developmental pathology are illustrated in Figure 8.

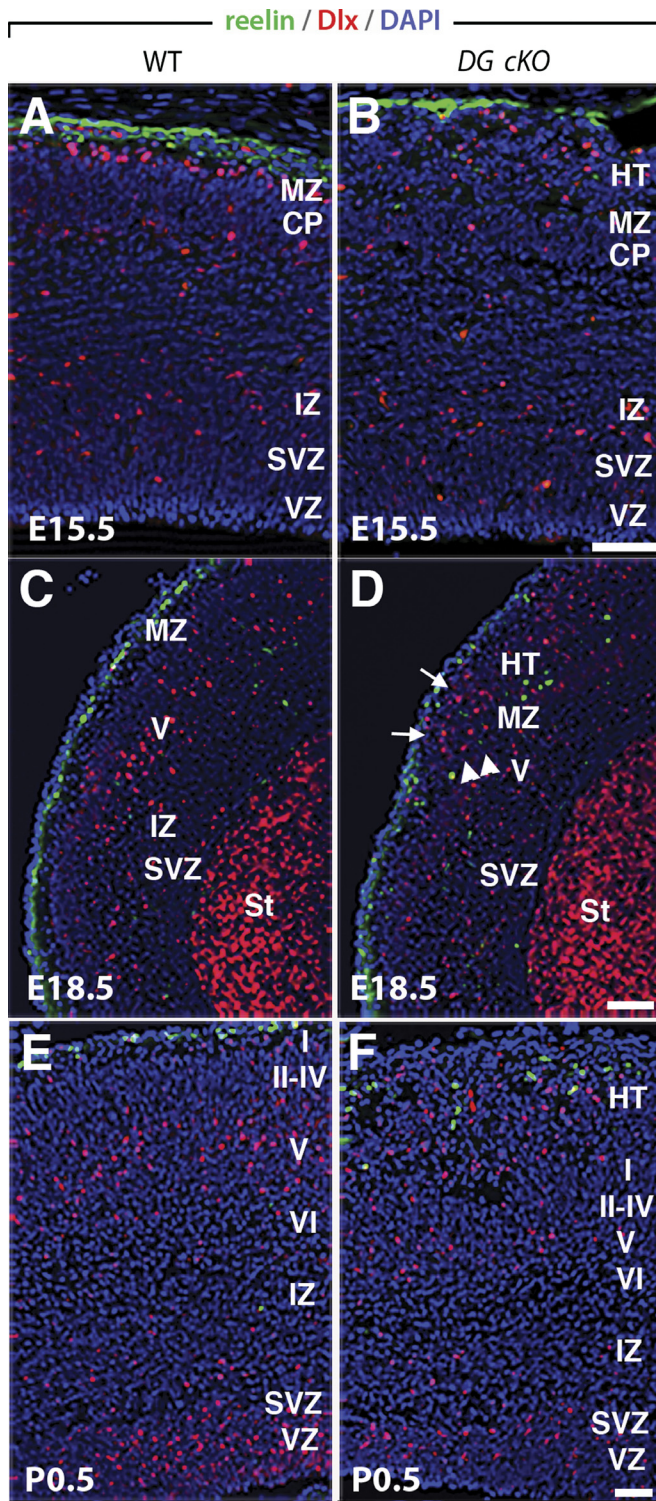
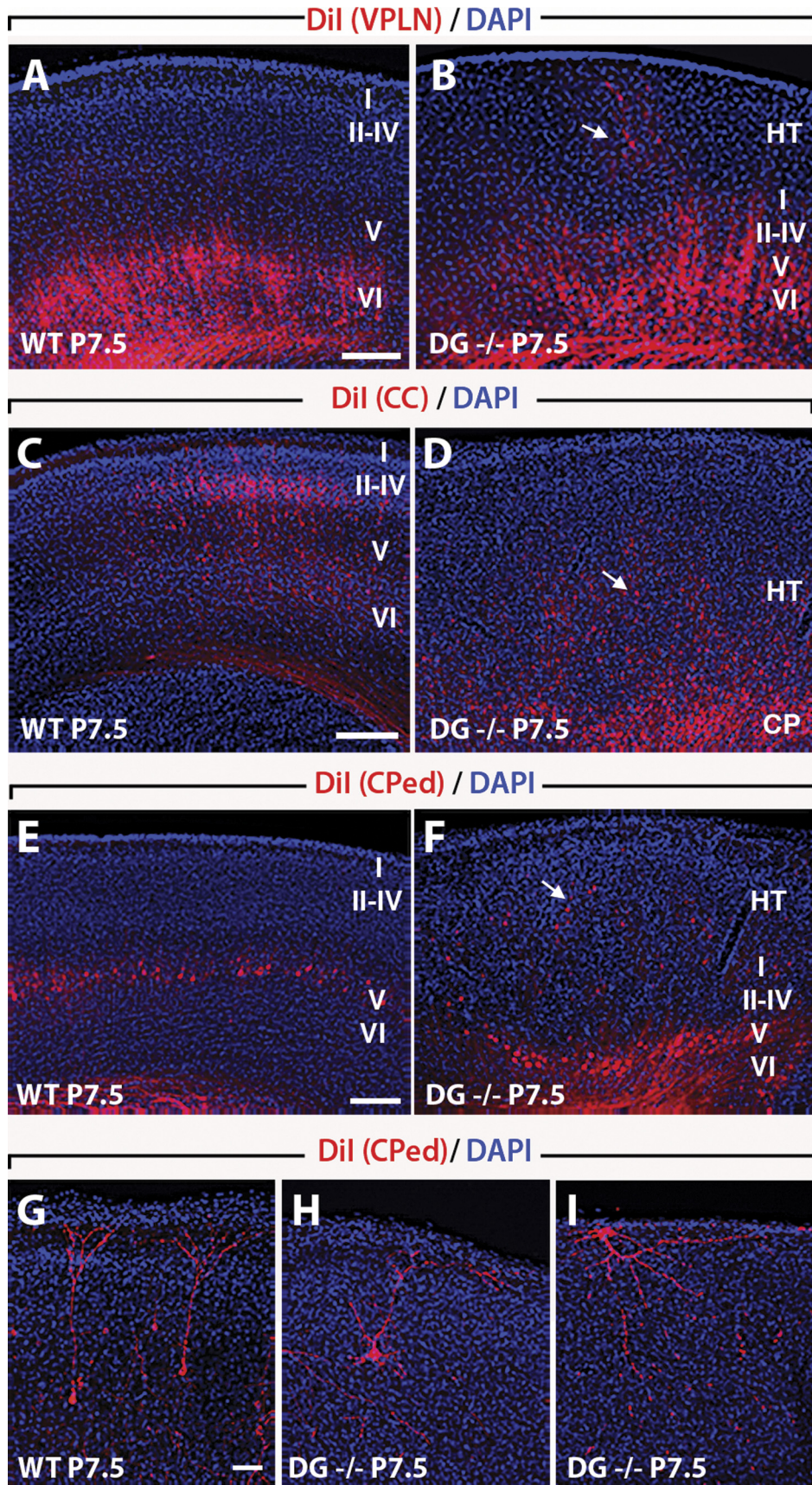


FIGURE 6. Interneurons migrate into meningeal heterotopia (HT). (A, B) In *Dag1*^{+/+} wild-type (WT) and *Dag1* cKO (*Dag1*^{-/-}) E15.5 brains, *Dlx*-positive interneurons migrate similarly from the ventral telencephalon to the CP in tangential migratory streams (arrows) from the ganglionic eminences. (C, D) Within the dorsal cortex, most *Dlx*-positive interneurons are in the MZ, IZ, and SVZ but are also present in HT of *Dag1* cKO brains (D). (E, F) In *Dag1*^{+/+} and *Dag1* cKO E18.5 brains, interneurons are tangentially migrating through lateral cortices in the IZ, SVZ, layer V, and the MZ (containing reelin-positive CR cells). In *Dag1* cKO brains, but not *Dag1*^{+/+} brains, many interneurons in the lateral cortex are in HT (arrows) overlying gaps in the reelin-positive CR cell monolayer (arrowheads) in the MZ (F). (G, H) By P0.5, many more interneurons are in the dorsal cortex compared with E15.5 in both *Dag1*^{+/+} and *Dag1* cKO brains. Most interneurons are in layer V, layer VI, the VZ, SVZ, and mixed with CR cells in layer I (G, H); however, large numbers of interneurons are also in HT of *Dag1* cKO brains (G). St, striatum. Scale bars = (A, B, E, F) 100 μm; (C, D, G, H) 50 μm.



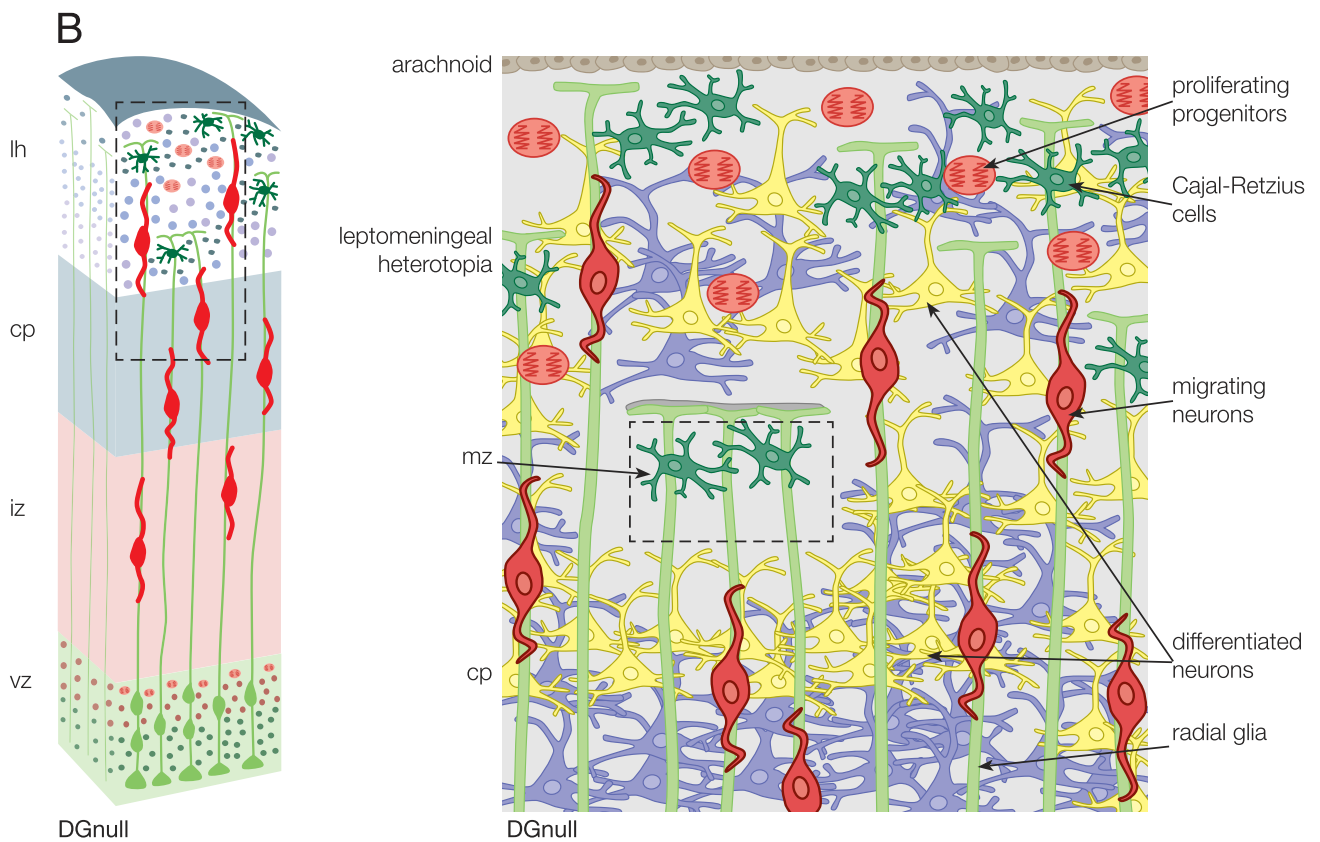
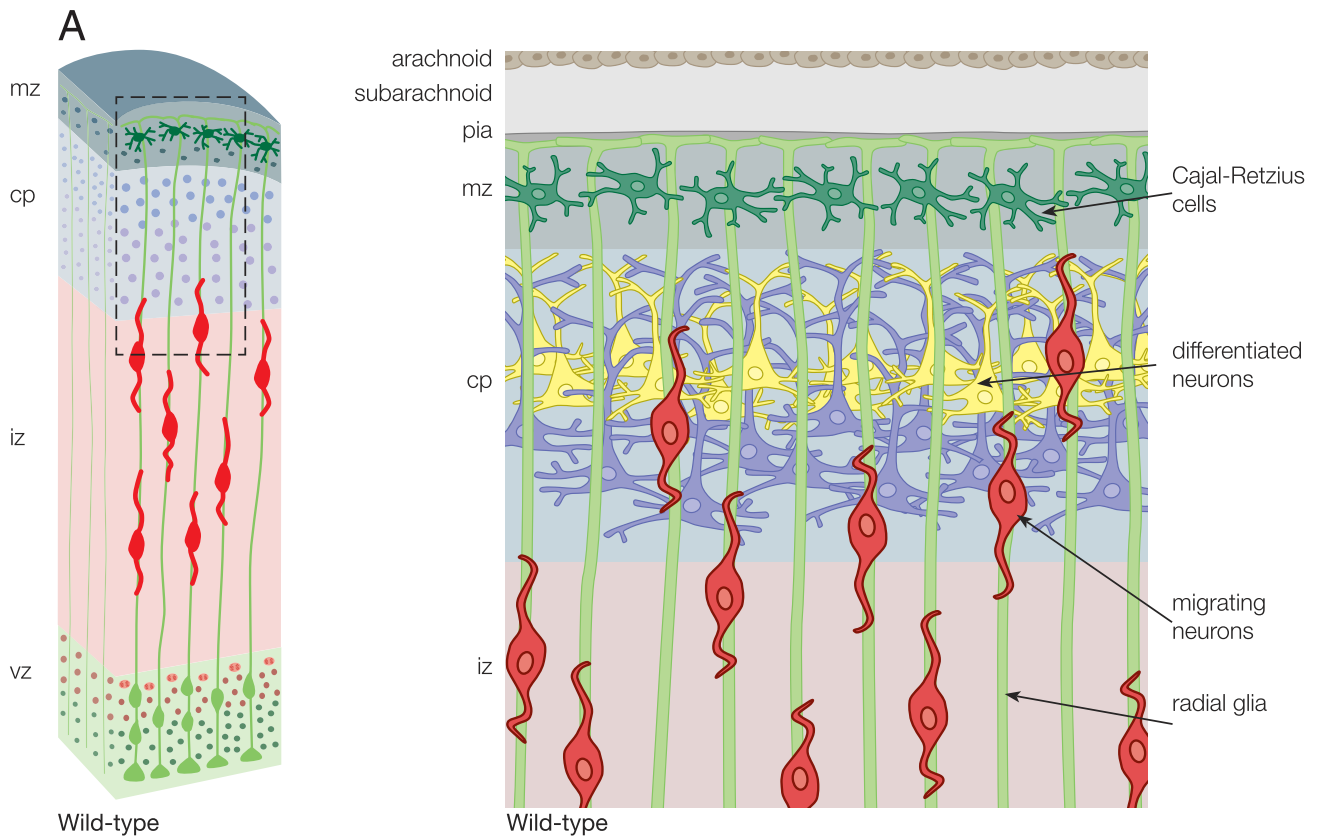
Consistent with previous findings in all cell types where DG is expressed as a major ECM receptor and is localized along the membrane where it contacts the basement membrane, *Dag1* mRNA expression colocalized with RG soma in the VZ during the neurogenic period, whereas DG protein was limited to RG basal process end feet where they interact with the PBM and establish the glia limitans. Radial glia are the only cell type that directly interface with the PBM during development, and localization of DG in RG end feet during neocortical histogenesis provides a basis for understanding the pathogenesis of neuronal migration disorders when DG absence results in the loss of necessary RG-PBM interactions. Absence of α - and β -DG from RG basal processes in *Dag1* cKO brains resulted in disarrayed and truncated RG fibers with subsequent loss of PBM throughout embryonic development. Radial glia basal processes normally provide a scaffold for some radially migrating projection neurons and interneurons (40, 71, 72), and the PBM normally compartmentalizes cortical neurons within the neocortical epithelium. Disarrayed RG fibers, breaches in the PBM, and RG fibers that extended into the meninges apparently facilitated overmigration of diverse cellular elements, including progenitor cells, CR cells, projection neurons, and interneurons, beyond the glia limitans and into meningeal spaces. Although the relative contribution of each remains unclear, progressive PBM disintegration, neuronal overmigration, and aberrant repair of the cortical surface throughout the embryonic period resulted in severe dyslamination and leptomeningeal heterotopia that were confluent with underlying residual cortices.

Cajal-Retzius cells migrated into the meninges soon after the PBM began to break down, leaving widespread gaps in the CR cell layer within the MZ. Reelin, which is produced by CR cells in the MZ, is an important positioning cue for radially migrating neurons and is necessary for establishment of the normal “inside-out” laminar pattern of the CP (73). Overmigration of CP neurons into the meninges may have been further facilitated by ectopic reelin within the developing meningeal heterotopia or by reduced reelin levels within the MZ, although it is unclear whether reelin acts as a “stop signal” during migration. Despite CR cells occasionally being distributed along the basal aspect of heterotopia, CP neurons rarely formed a laminar pattern in heterotopia. Instead, neurons with molecular phenotypes of different CP layers were typically admixed in heterotopia with no discernible pattern.

Neurons from all CP layers migrated into inappropriately superficial CP layers and into the meninges of *Dag1* cKO brains. Although not investigated in this study, the *Dag1* cKO brain could be used in future studies to examine the molecular mechanistic basis for neuronal overmigration after PBM disruption. Early-born neurons migrated into heterotopia soon after PBM discontinuities developed. However, by late embryogenesis, most heterotopic neurons expressed molecular phenotypes of late-born neurons destined for superficial CP layers. There was significant retention of normal CP lamination with early-born neurons even after widespread PBM disintegration was present in *Dag1* cKO brains. It is likely that cortical neurons have a window of opportunity for aberrant migration if permissive conditions such as loss of PBM integrity exist before becoming permanently settled in their laminar position. The time points when PBM disruptions first develop and the rate at which they progress in cobblestone lissencephaly likely impact the total number of neurons that migrate abnormally. Earlier or more rapid disintegration of the PBM may result in more extensive CP laminar disorganization and heterotopia formation because greater numbers of neurons may not yet have become fixed in their CP laminar position. A comparison of *Gfap-Cre* and *Nestin-Cre* *Dag1* cKO mice supports this hypothesis, that is, *Gfap-Cre* cKO mice lose DG approximately 2 to 3 days later than *Nestin-Cre* cKO mice and have less extensive cortical heterotopia. (74).

The clinical severity of neurologic deficits among humans with cobblestone lissencephaly varies widely, and this clinical heterogeneity seems to be associated at least in part with different known or unknown genetic mutations that result in hypoglycosylation of DG (75). Although not established in this study, we hypothesize that clinical phenotypic variability might be associated with mechanistic differences in DG hypoglycosylation that affect the rate and timing of PBM disruption and, therefore, the extent of cortical dysgenesis in cobblestone lissencephaly. This hypothesis could be further explored with comparative studies of mouse models of DG hypoglycosylation. Molecular and neuropathologic findings from a recent study of 65 fetal human cases provide support for this hypothesis (6). Interestingly, despite widespread disruption of the PBM, disarray of RG basal processes, and loss of many CR cells from the MZ of *Dag1* cKO brains by E16.5, many upper layer neurons successfully laminated in the CP after this time point. This suggests that factors other than PBM integrity, an orderly

FIGURE 7. Ectopic pyramidal neurons project to appropriate cortical and subcortical targets but have abnormal dendritic orientation. **(A, B)** In the somatosensory cortex of wild-type (WT) *Dag1*^{+/+} and *Dag1* cKO (*Dag1*^{-/-}) brains, layer VI neurons with thalamic projections are retrogradely labeled by Dil injections in the thalamic ventroposterior lateral nucleus (VPLN); however, ectopic layer VI neurons in superficial CP layers and heterotopic layer VI neurons **(B, arrow)** in *Dag1* cKO brains also established thalamic connections despite severe dyslamination. **(C, D)** In *Dag1*^{+/+} and *Dag1* cKO brains, neurons in all CP layers with commissural projections are retrogradely labeled by Dil injections in the corpus callosum. In *Dag1* cKO brains, many heterotopic neurons **(D, arrow)** also have commissural projections and are retrogradely labeled by Dil injections in the corpus callosum. **(E, F)** In *Dag1*^{+/+} and *Dag1* cKO brains, layer V neurons with subcerebral projections (to the brainstem and spinal cord) are retrogradely labeled by Dil injections in the cerebral peduncles. Many ectopic layer V neurons in superficial CP layers and heterotopia (HT) **(F, arrow)** also have subcerebral projections. **(G–I)** layer V pyramidal neurons in *Dag1*^{+/+} brains have parallel, radially oriented, apical dendrites ending in tufts in layer I **(G)**. Heterotopic neurons in *Dag1* cKO brains often have abnormally oriented and tortuous apical dendrites, which occasionally are bent against the outer edge of the HT **(H)** or are inverted **(I)**. Scale bars = **(A–F)** 200 μ m; **(G, I)** 100 μ m.



radial glial migratory scaffold, and normal spatial gradients of MZ reelin may contribute to appropriate lamination of some projection neurons.

Cortical projection neurons establish commissural and corticofugal connections with specific targets based on their molecular identity, which is normally highly correlated with laminar position (70). The development of appropriate cortical connections involves axon pathfinding mediated by extrinsic molecular signals in addition to reciprocal interactions with cortical afferent axons (70). Within the heterotopia of *Dag1* cKO brains, some pyramidal neurons showed altered polarity, including abnormally oriented or bent apical dendrites, closely resembling the morphology of neocortical neurons in humans with Walker-Warburg syndrome and cobblestone lissencephaly (76). Despite severe dyslamination and abnormal dendrite orientation, heterotopic pyramidal neurons established axonal connections with distant cortical and subcortical targets or projections within appropriate white matter tracts. This is consistent with the view that axon pathfinding does not require laminar organization. Extrinsic axonal pathfinding cues and intrinsic signals in ectopic cortical projection neurons were apparently sufficient for proper cortical projections independent of final laminar or heterotopic position. The plasticity of the developing cerebral cortex, as demonstrated by successful axon guidance despite extensive cortical dyslamination and abnormal dendrites of individual ectopic projection neurons in *Dag1* cKO brains, may also account in part for the high degree of retained neurologic function in some humans with cobblestone lissencephaly (75).

Pial basement membrane disintegration in *Dag1* cKO brains resulted in formation of meningeal neuronal heterotopia containing proliferating progenitor cells. Thus, the dystroglycanopathies with brain malformations are not only neuronal migration disorders but also progenitor migration disorders. Expression of the transcription factors Pax6 and Tbr2 is limited to RG and IPCs, the progenitors of glutamatergic neurons, in the dorsal telencephalon of normal mice. Radial glia and IPCs are normally restricted to the VZ and SVZ, respectively, during neocortical histogenesis. Ectopic Pax6-positive and Tbr2-positive cells in *Dag1* cKO brains were frequently immunoreactive for PCNA and PHH3 and incorporated BrdU, markers of proliferating cells, but were not immunoreactive for GFAP, a marker of astrocytic terminal differentiation. These ectopic Pax6-positive and Tbr2-positive cells were likely RG and IPCs that had lost both apical (ventricular) and basal (pial) attachments and migrated away from the VZ and SVZ. Remarkably, apical attachment and exposure to local extrinsic cues within

the neurogenic niches of the VZ and SVZ were therefore not essential for ectopic RG and IPCs to maintain proliferative progenitor phenotypes; however, the mechanism by which these phenotypes persist under these conditions and whether they eventually differentiate into terminal phenotypes remain unclear.

Mitotically active ectopic progenitor cells in superficial CP layers and heterotopia of *Dag1* cKO brains presumably produced ectopic glutamatergic neurons and thus contributed in part to dyslamination and expansion of heterotopic meningeal neuronal populations. Late in neurogenesis, most progenitor cells in normal murine neocortices are committed to produce upper layer neurons such as Cux1-positive cells (77). It is possible that ectopic progenitor cells in *Dag1* cKO brains, which were first detected relatively late in neurogenesis, produced mostly ectopic projection neurons expressing molecular markers of upper CP layers such as Cux1 because of their lineage restriction. This may partially contribute to the disparity in the number of early-born compared with late-born ectopic neurons that accumulated within meningeal heterotopia during late embryogenesis.

In summary, we verified that *Dag1* mRNA is expressed by RG cells in the embryonic VZ, whereas DG protein is localized to RG end feet in contact with the PBM, indicating that DG protein must be transported along the RG fiber to achieve this localization. We also found that *Dag1* inactivation led to disintegration of the PBM, RG fiber abnormalities, formation of heterotopia by aberrant migration of diverse cortical neuronal cell types into the meningeal space, and heterotopic proliferation of RG and IPC progenitor cells. Our findings demonstrate that DG expression on RG end feet is essential for multiple processes of neocortical histogenesis to occur normally. However, we also show that other developmental processes, such as establishment of appropriate axonal projections, can occur despite severe dyslamination and abnormal dendritic orientation. This study provides evidence that the pathogenesis of cobblestone malformation in dystroglycanopathy is associated with severe dyslamination of CP layers with aberrant migration of diverse cell types that are influenced by the timing and extent of PBM disruptions. It also demonstrates that cortical dysgenesis involves not only overmigration of neurons but also disturbances of RG morphology, progenitor distribution, and pyramidal neuron orientation.

ACKNOWLEDGMENT

The authors thank the investigators and laboratories listed in the Materials and Methods section for providing the antibodies.

FIGURE 8. Summary of abnormal neurogenesis in *Dag1* cKO model of dystroglycanopathy. **(A)** In wild-type (WT) brains **(A)**, neurons generated in the VZ and SVZ by RG and intermediate progenitor cells migrate through the IZ into the CP along the basal processes of RG. Radial glia basal processes terminate as foot processes on the PBM. Differentiated neurons form an inside-out laminar pattern in the CP below reelin-producing CR cells in the MZ and the PBM. **(B)** In DG-null brains, neurons generated in the VZ and SVZ migrate through the IZ into the CP and into the leptomeninges through discontinuities in the PBM. Proliferating heterotopic progenitor cells produce autochthonous heterotopic neurons. Radial glia basal processes extend into the leptomeninges through discontinuities in the PBM. There is profound cortical disorganization and formation of leptomeningeal heterotopia (lh) containing migrating neurons, differentiated neurons, CR cells, and proliferating progenitor cells. Residual intact PBM overlies small areas of normal CP.

REFERENCES

1. Comand B, Pihko H, Bayes M, et al. Clinical and genetic distinction between Walker-Warburg syndrome and muscle-eye-brain disease. *Neurology* 2001;56:1059–69
2. Haltia M, Leivo I, Somer H, et al. Muscle-eye-brain disease: A neuropathological study. *Ann Neurol* 1997;41:173–80
3. Fukuyama Y, Osawa M, Suzuki H. Congenital progressive muscular dystrophy of the Fukuyama type—clinical, genetic, and pathological considerations. *Brain Dev* 1981;3:1–29
4. Pang T, Atefy R, Sheen V. Malformations of cortical development. *Neurologist* 2008;14:181–91
5. Golden JA. Cell migration and cerebral cortical development. *Neuropathol Appl Neurobiol* 2001;27:22–28
6. Devisme L, Bouchet C, Gonzales M, et al. Cobblestone lissencephaly: Neuropathological subtypes and correlations with genes of dystroglycanopathies. *Brain* 2012;135:469–82
7. Liu J, Ball SL, Yang Y, et al. A genetic model for muscle-eye-brain disease in mice lacking protein *O*-mannose 1,2-*N*-acetylglucosaminyltransferase (POMGnT1). *Mech Dev* 2006;123:228–40
8. Chiyonobu T, Sasaki J, Nagai Y, et al. Effects of fukutin deficiency in the developing mouse brain. *Neuromuscul Disord* 2005;15:416–26
9. Hu H, Yang Y, Eade A, et al. Breaches of the pial basement membrane and disappearance of the glia limitans during development underlie the cortical lamination defect in the mouse model of muscle-eye-brain disease. *J Comp Neurol* 2007;501:168–83
10. Dobyns WB, Pagon RA, Armstrong D, et al. Diagnostic criteria for Walker-Warburg syndrome. *Am J Med Genet* 1989;32:195–210
11. Santavuori P, Somer H, Sainio K, et al. Muscle-eye-brain disease (MEB). *Brain Dev* 1989;11:147–53
12. Fukuyama Y, Osawa M, Suzuki H. Congenital progressive muscular dystrophy of the Fukuyama type—Clinical, genetic, and pathological considerations. *Brain Dev* 1981;3:1–29
13. Nakano I, Funahashi M, Takada K, et al. Are breaches in the glia limitans the primary cause of the micropolygyria in Fukuyama-type congenital muscular dystrophy (FCMD)? Pathological study of the cerebral cortex of an FCMD fetus. *Acta Neuropathol* 1996;91:313–21
14. Moore SA, Saito F, Chen J, et al. Deletion of brain dystroglycan recapitulates aspects of congenital muscular dystrophy. *Nature* 2002;418:422–25
15. Michele DE, Barresi R, Kanagawa M, et al. Post-translational disruption of dystroglycan-ligand interactions in congenital muscular dystrophies. *Nature* 2002;418:417–22
16. Kim DS, Hayashi YK, Matsumoto H, et al. POMT1 mutation results in defective glycosylation and loss of laminin-binding activity in alpha-DG. *Neurology* 2004;62:1009–11
17. Schachter H, Vajsar J, Zhang W. The role of defective glycosylation in congenital muscular dystrophy. *Glycoconj J* 2004;20:291–300
18. Grewal PK, Hewitt JE. Glycosylation defects: A new mechanism for muscular dystrophy? *Hum Mol Genet* 2003;12(R2):R259–64
19. Beltrán-Valero de Bernabé D, Currier S, Steinbrecher A, et al. Mutations in the *O*-mannosyltransferase gene POMT1 give rise to the severe neuronal migration disorder Walker-Warburg syndrome. *Am J Hum Genet* 2002;71:1033–43
20. Yoshida A, Kobayashi K, Manya H, et al. Muscular dystrophy and neuronal migration disorder caused by mutations in a glycosyltransferase, POMGnT1. *Dev Cell* 2001;1:17–24
21. van Recesswijk J, Janssen M, van den Elzen C, et al. POMT2 mutations cause alpha-dystroglycan hypoglycosylation and Walker Warburg syndrome. *J Med Genet* 2005;42:907–12
22. Henry MD, Campbell KP. A role for dystroglycan in basement membrane assembly. *Cell* 1998;95:859–70
23. Henry MD, Satz JS, Brakebusch C, et al. Distinct roles for dystroglycan, beta1 integrin and perlecan in cell surface laminin organization. *J Cell Sci* 2001;114:1137–44
24. Halfter W, Dong S, Yip Y-P, et al. A critical function of the pial basement membrane in cortical histogenesis. *J Neurosci* 2002;22:6029–40
25. Graus-Porta D, Blaess S, Senften M, et al. β 1-class integrins regulate the development of laminae and folia in the cerebral and cerebellar cortex. *Neuron* 2001;31:367–79
26. Beggs HE, Schahin-Reed D, Zang K, et al. FAK deficiency in cells contributing to the basal lamina results in cortical abnormalities resembling congenital muscular dystrophies. *Neuron* 2003;40:501–14
27. Niewmierzycka A, Mills J, St-Arnaud R, et al. Integrin-linked kinase deletion from mouse cortex results in cortical lamination defects resembling cobblestone lissencephaly. *J Neurosci* 2005;25:7022–31
28. Georges-Labouesse E, Mark M, Messaddeq N, et al. Essential role of α 6 integrins in cortical and retinal lamination. *Curr Biol* 1998;8:983–86
29. Satz JS, Philp AR, Kusano H, et al. Visual impairment in the absence of dystroglycan. *J Neurosci* 2009;29:13136–46
30. Williamson RA, Henry MD, Daniels KJ, et al. Dystroglycan is essential for early embryonic development: Disruption of Reichert's membrane in *Dag1*-null mice. *Hum Mol Genet* 1997;6:831–41
31. Satz JS, Barresi R, Durbejj M, et al. Brain and eye malformations resembling Walker-Warburg syndrome are recapitulated in mice by dystroglycan deletion in the epiblast. *J Neurosci* 2008;28:10567–75
32. Tronche F, Kellendonk C, Kretz O, et al. Disruption of the glucocorticoid receptor gene in the nervous system results in reduced anxiety. *Nat Genet* 1999;23:99–103
33. Duclos F, Straub V, Moore SA, et al. Progressive muscular dystrophy in alpha-sarcoglycan-deficient mice. *J Cell Biol* 1998;142:1461–71
34. Bulfone A, Martinez S, Marigo V, et al. Expression pattern of the *Tbr2* (cohesoderm) gene during mouse and chick brain development. *Mech Dev* 1999;84:133–38
35. Gotz M, Stoykova A, Gruss P. Pax6 controls radial glia differentiation in the cerebral cortex. *Neuron* 1998;21:1031–44
36. Englund C, Fink A, Lau C, et al. Pax6, Tbr2, and Tbr1 are expressed sequentially by radial glia, intermediate progenitor cells, and postmitotic neurons in developing neocortex. *J Neurosci* 2005;25:247–51
37. Holt KH, Crosbie RH, Venzke DP, et al. Biosynthesis of dystroglycan: Processing of a precursor propeptide. *FEBS Lett* 2000;468:79–83
38. Zaccaria ML, Di Tommaso F, Brancaccio A, et al. Dystroglycan distribution in adult mouse brain: A light and electron microscopy study. *Neurosci* 2001;104:311–24
39. Misson JP, Edwards MA, Yamamoto M, et al. Identification of radial glial cells within the developing murine central nervous system: Studies based upon a new immunohistochemical marker. *Brain Res Dev Brain Res* 1988;44:95–108
40. Rakic P. Mode of cell migration to the superficial layers of fetal monkey neocortex. *J Comp Neurol* 1972;145:61–83
41. Kriegstein AR, Noctor SC. Patterns of neuronal migration in the embryonic cortex. *Trends Neurosci* 2004;27:392–99
42. Muzumdar D, Michaud J, Ventureyra EC. Anterior cranial base glioneuronal heterotopia. *Childs Nerv Syst* 2006;22:227–33
43. Oya S, Kawahara N, Aoki S, et al. Intracranial extracerebral glioneuronal heterotopia. Case report and review of the literature. *J Neurosci* 2005;102:105–12
44. Kershnik MM, Kaplan C, Craven CM, et al. Intrapulmonary neuroglial heterotopia. *Arch Pathol Lab Med* 1992;116:1043–46
45. Juric-Sekhar G, Kapur RP, Glass IA, et al. Neuronal migration disorders in microcephalic osteodysplastic primordial dwarfism type I/III. *Acta Neuropathol* 2011;121:545–54
46. Eriksson SH, Thom M, Heffernan J, et al. Persistent reelin-expressing Cajal-Retzius cells in polymicrogyria. *Brain* 2001;124:1350–61
47. Komatsu S, Sakata-Haga H, Sawada K, et al. Prenatal exposure to ethanol induces leptomeningeal heterotopia in the cerebral cortex of the rat fetus. *Acta Neuropathol* 2001;101:22–26
48. Hendzel MJ, Wei Y, Mancini MA, et al. Mitosis-specific phosphorylation of histone H3 initiates primarily within pericentromeric heterochromatin during G2 and spreads in an ordered fashion coincident with mitotic chromosome condensation. *Chromosoma* 1997;106:348–60
49. McKeever PE. Insights about brain tumors gained through immunohistochemistry and in situ hybridization of nuclear and phenotypic markers. *J Histochem Cytochem* 1998;46:585–94
50. Hevner RF. Layer-specific markers as probes for neuron type identity in human neocortex and malformations of cortical development. *J Neuropathol Exp Neurol* 2007;66:101–9
51. D'Arcangelo G, Nakajima K, Miyata T, et al. Reelin is a secreted glycoprotein recognized by the CR-50 monoclonal antibody. *J Neurosci* 1997;17:23–31
52. Hammond V, Howell B, Godinho L, et al. Disabled-1 functions cell autonomously during radial migration and cortical layering of pyramidal neurons. *J Neurosci* 2001;21:8798–808

53. Arlotta P, Molyneaux BJ, Chen J, et al. Neuronal subtype-specific genes that control corticospinal motor neuron development in vivo. *Neuron* 2005;45:207–21
54. Hevner RF, Shi L, Justice N, et al. *Tbr1* regulates differentiation of the preplate and layer 6. *Neuron* 2001;29:353–66
55. Hevner RF, Daza RAM, Rubenstein JLR, et al. Beyond laminar fate: Toward a molecular classification of cortical projection/pyramidal neurons. *Dev Neurosci* 2003;25:139–51
56. Molnar Z, Cheung AFP. Towards the classification of subpopulations of layer V pyramidal projection neurons. *Neurosci Res* 2006;55:105–15
57. Yoneshima H, Yamasaki S, Voelker CCJ, et al. ER81 is expressed in a subpopulation of layer 5 neurons in rodent and primate neocortices. *Neurosci* 2006;137:401–12
58. Schaeren-Wiemers N, Andre E, Kapfhammer JP, et al. The expression pattern of the orphan nuclear receptor Ror β in the developing and adult rat nervous system suggests a role in the processing of sensory information and in circadian rhythm. *Eur J Neurosci* 1997;9:2687–701
59. Nieto M, Monuki ES, Tang H, et al. Expression of Cux-1 and Cux-2 in the subventricular zone and upper layers II–IV of the cerebral cortex. *J Comp Neurol* 2004;479:168–80
60. Angevine JB, Sidman RL. Autoradiographic study of cell migration during histogenesis of cerebral cortex in the mouse. *Nature* 1961;192:766–68
61. Rakic P. Neurons in rhesus monkey visual cortex: Systematic relation between time of origin and eventual disposition. *Science* 1974;183:425–27
62. Pleasure SJ, Anderson S, Hevner R, et al. Cell migration from the ganglionic eminences is required for the development of hippocampal GABAergic interneurons. *Neuron* 2000;28:727–40
63. Anderson SA, Eisenstat DD, Shi L, et al. Interneuron migration from basal forebrain to neocortex: Dependence on *Dlx* genes. *Science* 1997;278:474–76
64. Ang ESBC Jr, Haydar TF, Gluncic V, et al. Four-dimensional migratory coordinates of GABAergic interneurons in the developing mouse cortex. *J Neurosci* 2003;23:5805–15
65. Fairen A, Cobas A, Fonseca M. Times of generation of glutamic acid decarboxylase immunoreactive neurons in mouse somatosensory cortex. *J Comp Neurol* 1986;251:67–83
66. Peduzzi JD. Genesis of GABA-immunoreactive neurons in the ferret visual cortex. *J Neurosci* 1988;8:920–31
67. Hevner RF, Daza RAM, Englund C, et al. Postnatal shifts of interneuron position in the neocortex of normal and reeler mice: Evidence for inward radial migration. *Neurosci* 2004;124:605–18
68. Gotz M, Huttner WB. The cell biology of neurogenesis. *Nat Rev Mol Cell Biol* 2005;6:777–88
69. Pilz D, Stoodley N, Golden JA. Neuronal migration, cerebral cortical development, and cerebral cortical anomalies. *J Neuropathol Exp Neurol* 2002;61:1–11
70. Price DJ, Kennedy H, Dehay C, et al. The development of cortical connections. *Eur J Neurosci* 2006;23:910–20
71. Misson JP, Austin CP, Takahashi T, et al. The alignment of migrating neural cells in relation to the murine neopallial radial glial fiber system. *Cereb Cortex* 1991;1:221–29
72. Poluch S, Juliano SL. A normal radial glial scaffold is necessary for migration of interneurons during neocortical development. *Glia* 2007;55:822–30
73. Ogawa M, Miyata T, Nakajima K, et al. The reeler gene-associated antigen on Cajal-Retzius neurons is a crucial molecule for laminar organization of cortical neurons. *Neuron* 1995;14:899–912
74. Satz JS, Ostendorf AP, Hou S, et al. Distinct functions of glial and neuronal dystroglycan in the developing and adult mouse brain. *J Neurosci* 2010;30:14560–72
75. Godfrey C, Clement E, Mein R, et al. Refining genotype-phenotype correlations in muscular dystrophies with defective glycosylation of dystroglycan. *Brain* 2007;130:2725–35
76. Judas M, Sedmak G, Rados M, et al. POMT1-Associated Walker-Warburg syndrome: A disorder of dendritic development of neocortical neurons. *Neuropediatrics* 2009;40:6–14
77. Frantz GD, McConnell SK. Restriction of late cerebral cortical progenitors to an upper layer fate. *Neuron* 1996;17:55–61